Chemistry & Biology
Article

Highly Selective Inhibitors of Monoacylglycerol Lipase Bearing a Reactive Group that Is Bioisosteric with Endocannabinoid Substrates

Jae Won Chang,[1,3] Micah J. Niphakis,[1,3,*] Kenneth M. Lum,[1] Armand B. Cognetta, III,[1] Chu Wang,[1] Megan L. Matthews,[1] Sherry Niessen,[1] Matthew W. Buczynski,[2] Loren H. Parsons,[2] and Benjamin F. Cravatt[1,*]
[1]The Skaggs Institute for Chemical Biology and Department of Chemical Physiology
[2]Committee of Neurobiology of Addictive Disorders
The Scripps Research Institute, La Jolla, CA 92037, USA
[3]These authors contributed equally to this work
*Correspondence: mniphak@scripps.edu (M.J.N.), cravatt@scripps.edu (B.F.C.)
DOI 10.1016/j.chembiol.2012.03.009

SUMMARY

The endocannabinoids 2-arachidonoyl glycerol (2-AG) and *N*-arachidonoyl ethanolamine (anandamide) are principally degraded by monoacylglycerol lipase (MAGL) and fatty acid amide hydrolase (FAAH), respectively. The recent discovery of *O*-aryl carbamates such as JZL184 as selective MAGL inhibitors has enabled functional investigation of 2-AG signaling pathways in vivo. Nonetheless, JZL184 and other reported MAGL inhibitors still display low-level cross-reactivity with FAAH and peripheral carboxylesterases, which can complicate their use in certain biological studies. Here, we report a distinct class of *O*-hexafluoroisopropyl (HFIP) carbamates that inhibits MAGL in vitro and in vivo with excellent potency and greatly improved selectivity, including showing no detectable cross-reactivity with FAAH. These findings designate HFIP carbamates as a versatile chemotype for inhibiting MAGL and should encourage the pursuit of other serine hydrolase inhibitors that bear reactive groups resembling the structures of natural substrates.

INTRODUCTION

Endocannabinoids are lipid transmitters that serve as endogenous ligands for the cannabinoid receptors CB1 and CB2, which are also activated by Δ^9-tetrahydrocannabinol, the psychoactive ingredient of marijuana. The two major endocannabinoids, 2-arachidonoyl glycerol (2-AG) and *N*-arachidonoyl ethanolamine (anandamide or AEA), play important roles in a wide range of physiological and pathological processes, including pain, cognition, emotionality, and feeding (Ligresti et al., 2009; Graham et al., 2009; Di Marzo, 2008, 2009; De Petrocellis and Di Marzo, 2009; Fowler, 2008; Ahn et al., 2008; Guindon et al., 2011). The signaling functions of 2-AG and AEA are terminated by enzymatic hydrolysis in processes principally mediated by the serine hydrolases monoacylglycerol lipase (MAGL) and fatty acid amide hydrolase (FAAH), respectively (Ahn et al., 2008). Additional 2-AG hydrolases exist, such as ABHD6 and ABHD12, and these enzymes may also regulate specific endocannabinoid pathways in vivo (Blankman et al., 2007; Marrs et al., 2010).

Pharmacologic and/or genetic disruption of MAGL and FAAH has provided evidence that elevations in endocannabinoid signaling can produce an intriguing subset of the behavioral effects of direct CB1 agonists. FAAH$^{(-/-)}$ mice or rodents treated with FAAH inhibitors, for instance, show antihyperalgesia and antianxiety/depression without exhibiting psychotropic responses or deficits in motor function (Cravatt et al., 2001; Lichtman et al., 2004; Kathuria et al., 2003; Ahn et al., 2009). MAGL inhibitors show a similar, but somewhat broader spectrum of CB1-dependent behavioral effects (Long et al., 2009a), and, at high doses, can lead to desensitization and downregulation of CB1 receptors (Schlosburg et al., 2010). Dual FAAH/MAGL inhibitors, on the other hand, promote cataleptic and drug-dependence behaviors in mice that are more reminiscent of direct CB1 agonists (Long et al., 2009c). These data designate selective FAAH and MAGL inhibitors as useful probes for dissecting the functions of different branches of the endocannabinoid system and as potential therapeutic agents for treating pain and neuropsychiatric disorders. However, the results also underscore the importance of maintaining high levels of selectivity to avoid simultaneous blockade of both FAAH and MAGL.

Lead MAGL inhibitors from the *O*-aryl carbamate class, such as JZL184, which inactivate MAGL by covalent carbamylation of the enzyme's serine nucleophile, show good selectivity (>100-fold) for MAGL over FAAH, ABHD6, and most other serine hydrolases (Long et al., 2009a, 2010). However, we have found that the residual, low-level cross-reactivity displayed by JZL184 for FAAH does lead to partial inhibition of this enzyme following high-dosing and chronic treatment regimens (Long et al., 2009a, 2009b; Schlosburg et al., 2010). Thus, a need remains to identify inhibitors that show more complete selectivity for MAGL over FAAH to avoid the potentially confounding effects of dual activation of 2-AG and AEA pathways in vivo. Here, we report the discovery and characterization of structurally distinct carbamate inhibitors bearing a hexafluoroisopropanol-leaving group that act as highly selective and in vivo-active inhibitors of MAGL. Competitive activity-based protein profiling (ABPP) and endocannabinoid-specific biomarker assays confirmed

that a *O*-hexafluoroisopropyl (HFIP) carbamate analog of JZL184, here named KML29, potently and selectively inhibited MAGL in vitro and in vivo with minimal cross-reactivity toward other central and peripheral serine hydrolases, including no detectable activity against FAAH.

RESULTS

Discovery of HFIP Carbamates as Selective MAGL Inhibitors

In our search for new classes of inhibitors that might display improved selectivity for MAGL over FAAH, we sought to replace the *p*-nitrophenol leaving group of JZL184 with another electrophilic moiety that better discriminated between these two endocannabinoid hydrolases. We were particularly attracted to hexafluoroisopropanol as a leaving group because it possesses a low pKa value (~9.3) and a structure that resembles the glycerol of MAGL's natural substrates (Figure 1A). It is furthermore known that modification of the methylene proximal to the amide on AEA impairs FAAH hydrolysis (Figure 1A) (Lang et al., 1999). We therefore reasoned that HFIP carbamates might retain excellent activity against MAGL while, at the same time, exhibiting reduced inhibition of FAAH. We synthesized HFIP carbamate analogs for three known endocannabinoid hydrolase inhibitors: the MAGL-selective inhibitor JZL184 (KML29, Figure 1A) (Long et al., 2009a, 2010); the ABHD6-selective inhibitor WWL70 (JW618, Figure 1A) (Li et al., 2007); and the dual MAGL/FAAH inhibitor JZL195 (JW642, Figure 1A) (Long et al., 2009c, 2010).

We initially assayed each HFIP carbamate for inhibition against MAGL, FAAH, ABHD6, and other mouse brain serine hydrolases using competitive ABPP (Leung et al., 2003). In this assay, cell or tissue proteomes are treated with inhibitors followed by the serine hydrolase-directed activity-based probe fluorophosphonate-rhodamine (FP-Rh), and inhibition is recorded as a reduction in FP-Rh probe labeling of individual serine hydrolases following separation by SDS-PAGE and in-gel fluorescence scanning. Competitive ABPP gels of mouse brain membrane proteome revealed that HFIP carbamates exhibit outstanding selectivity for MAGL over FAAH compared to the corresponding *O*-aryl carbamates (Figure 1B; Table 1; and see Figure S1 available online). The HFIP analog of JZL184, KML29, for instance, showed complete selectivity for MAGL over FAAH across the concentration range tested (0.001–50 μM) and greater than 100-fold selectivity for ABHD6, the only observable off target in the mouse brain proteome (Figure 1C; Table 1). This improvement in selectivity came without any sacrifice in potency because KML29 and JZL184 were found to exhibit equivalent IC_{50} values for MAGL inhibition (Table 1). Similar results were obtained using 2-AG and AEA substrate assays, which confirmed that KML29 is a potent inhibitor of 2-AG hydrolysis, but did not affect AEA hydrolysis at any concentration tested (Figure 1D). JW618, the HFIP analog of the selective ABHD6 inhibitor WWL70 (Li et al., 2007), acted as a dual MAGL/ABHD6 inhibitor with no detectable cross-reactivity with FAAH (Figure 1B; Table 1). Finally, and perhaps most surprisingly, JW642, the HFIP analog of the low nanomolar dual MAGL/FAAH inhibitor JZL195, inhibited MAGL with >1,000-fold greater potency than FAAH, indicating that simple replacement of the *p*-nitrophenyl group with the HFIP group was sufficient to convert potent dual FAAH/MAGL inhibitors into agents that displayed high selectivity for MAGL. That the selectivities displayed by KML29 and JW642 for MAGL over ABHD6 were nearly equivalent to those observed for their parent *p*-nitrophenyl carbamates indicates that the HFIP group is accommodated equally well by both of these enzymes, consistent with their shared ability to hydrolyze the substrate analog 2-AG.

To gain further insight into the mode of inhibition of MAGL by HFIP carbamates, we first determined by mass spectrometry analysis that KML29 reacts with the catalytic serine nucleophile of MAGL to form a stable, carbamylated adduct (Figures 2A and 2B). This covalent mechanism of inhibition mirrors that of the *p*-nitrophenoxy carbamate JZL184 (Long et al., 2009b). We also modeled the binding of KML29 to the MAGL active site using recently described crystal structures of the human MAGL (hMAGL) enzyme (Bertrand et al., 2010). The resulting model provided evidence that the HFIP group of KML29 could bind to MAGL in a similar manner to that predicted for the glycerol moiety of 2-AG (Bertrand et al., 2010), including potential interactions with the conserved active site residues His121 and Tyr194 (Figure 2C). Together, these data demonstrate that HFIP carbamates can serve as potent and selective inhibitors of MAGL and possibly other 2-AG hydrolases.

KML29 Selectively Inhibits MAGL in Mice

Having demonstrated that KML29 is a potent and selective MAGL inhibitor in vitro, we next evaluated the activity of this compound in vivo. C57Bl/6 mice were treated with a dose range (1–40 mg kg^{-1}, p.o.) of KML29 or JZL184, or vehicle, and after 4 hr were sacrificed, and their tissues removed and analyzed by competitive ABPP to assess serine hydrolase activities (Figure 3A). KML29 and JZL184 showed comparable dose-dependent blockade of MAGL activity in brain, with partial inhibition observed at 5 mg kg^{-1} and maximal inhibition achieved by 20 mg kg^{-1}. Consistent with the in vitro selectivity profile for each inhibitor, JZL184 was found to partially inhibit FAAH at the highest dose tested (40 mg kg^{-1}), whereas KML29 exhibited complete selectivity over FAAH at all doses tested. Similar profiles were generated for KML29 when administered to mice intraperitoneally (i.p.) (Figure S2). We have previously noted that the limited solubility of JZL184 necessitates sonication in the chosen vehicle prior to administration. Prolonged sonication and mild heating were also required for the dissolution of KML29 in vehicles for p.o. (PEG) or i.p. (saline:emulphor:ethanol [18:1:1]) routes of administration (see Experimental Procedures for details).

Consistent with the dose-dependent inhibition of MAGL observed by competitive ABPP, KML29 produced significant elevations in brain 2-AG at doses as low as 5 mg kg^{-1}, and these increases peaked at ~10-fold over vehicle controls at the 20 and 40 mg kg^{-1} doses (Figure 3B). As previously reported for other MAGL inhibitors (Long et al., 2009a, 2009b) and $MAGL^{(-/-)}$ mice (Schlosburg et al., 2010), we observed, concomitant with 2-AG elevations, significant reductions in brain arachidonic acid (AA). In contrast, brain levels for the endogenous FAAH substrates AEA, *N*-palmitoylethanolamine (PEA), and *N*-oleoylethanolamine (OEA) were unaltered by KML29 treatment at all tested doses (Figure 3B). Finally, we measured residual MAGL

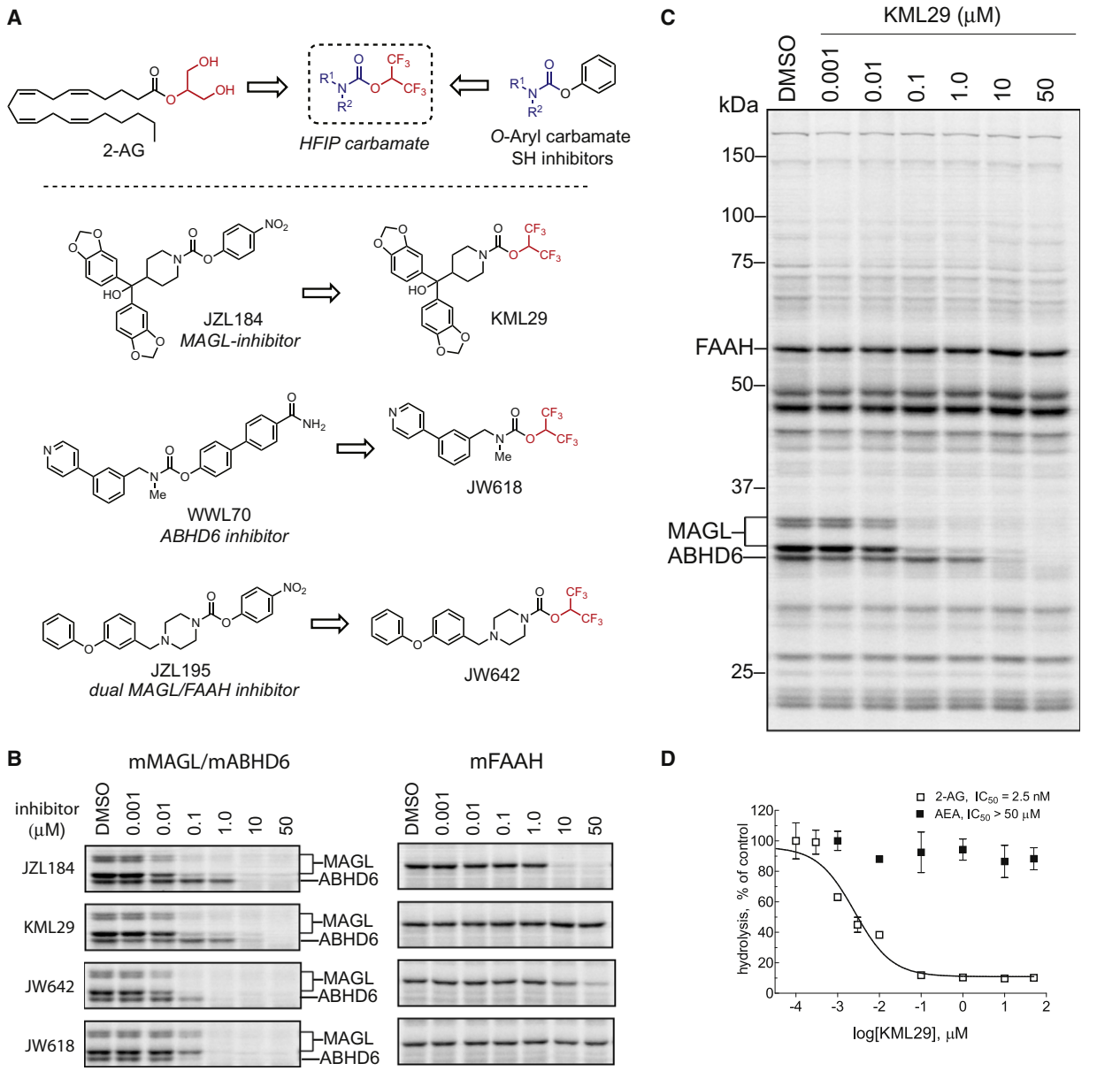

Figure 1. Discovery of HFIP Carbamates as Potent and Selective MAGL Inhibitors

(A) Structures of 2-AG, representative *O*-aryl carbamate inhibitors of endocannabinoid hydrolases, and HFIP carbamate analogs of these inhibitors, showing the bioisosteric nature of the HFIP group compared to the glycerol head group of MAGL substrate 2-AG.

(B) Competitive ABPP gels comparing the potency and selectivity of JZL184, KML29, JW642, and JW618 against MAGL, ABHD6, and FAAH in mouse brain proteomes. See Figure S1 for full gel profiles of each inhibitor. See also Table 1 for IC_{50} values calculated from gel-based ABPP experiments. Note that MAGL migrates as two bands in the mouse brain likely due to alternative spliced isoforms (Karlsson et al., 2001).

(C) Full competitive ABPP gel showing KML29 activity against mouse brain serine hydrolase activities, which revealed selective inhibition of MAGL at concentrations up to 1 μM and ABHD6 inhibition as the only off target at inhibitor concentrations up to 50 μM.

(D) Blockade of MAGL and FAAH by KML29 in mouse brain proteomes as measured by hydrolysis of 2-AG and AEA, respectively. Data are presented as mean ± SEM of three independent experiments.

Gels are representative images from three independent experiments (n = 3).

See also Figure S1.

and FAAH activity in brain proteomes from KML29-treated mice using substrate assays (Figure 3B), which confirmed the dose-dependent inhibition of MAGL and the lack of any effect on FAAH.

We also evaluated the duration of action of KML29 in vivo by assessing MAGL activity at various time points following a single, oral dose of the inhibitor (20 mg kg^{-1}) (Figure S2). As has been reported previously for JZL184 (Long et al., 2009a), KML29

Table 1. IC_{50} Values for JZL184 and HFIP Carbamates against Mouse, Rat, and Human Orthologs of MAGL, FAAH, and ABHD6

	Inhibitor IC_{50} (nM)			
	JZL184	KML29	JW642	JW618
Mouse				
MAGL	10[a]	15 (11–21)	7.6 (5.5–10)	123 (91–160)
FAAH	4,690[a]	>50,000	31,000 (22,700–44,100)	>50,000
ABHD6	3,270[a]	4,870 (4,120–5,760)	107 (41–285)	38 (29–50)
Rat				
MAGL	262 (188–363)	43 (36–52)	14 (13–16)	385 (329–451)
FAAH	3,570 (2,540–5,020)	>50,000	14,000 (12,300–17,000)	>50,000
ABHD6	2,940 (1,441–6,010)	1,600 (1,260–2,040)	50 (32–78)	13 (8.9–18)
Human				
MAGL	3.9 (1.8–8.1)	5.9 (4.0–9.9)	3.7 (2.3–5.9)	6.9 (4.4–11)
FAAH	>50,000	>50,000	20,600 (13,000–32,600)	>50,000

Serine hydrolase inhibition was measured by competitive ABPP where reductions in FP-Rh labeling of MAGL, ABHD6, and FAAH were quantified following preincubation of proteomic samples with the indicated inhibitor. Brain membrane proteomes were used to measure inhibition of mouse and rat enzymes, whereas human enzymes were evaluated from proteomes of transiently transfected HEK293T cells. IC_{50} values are reported as the mean from three independent experiments. The 95% confidence intervals are listed in the parentheses.
See also Figures S1 and S3.
[a]Previously determined IC_{50} values (Long et al., 2010).

caused maximal inhibition of MAGL in the brain by 1 hr post-administration, the earliest time point tested. This inhibition was sustained until 12–24 hr, at which times MAGL activity began to return to control levels. Importantly, KML29 maintained complete selectivity for MAGL over FAAH for the duration of the time course experiment. Brain lipid profiles for 2-AG, AA, and AEA corroborated these gel profiles, revealing maximal elevations of 2-AG and reductions of AA at 1 hr followed by a gradual return toward basal levels over the 24 hr time course. AEA levels, on the other hand, were unaltered throughout the 24 hr period.

In addition to showing low-level cross-reactivity with FAAH, JZL184 also inhibits a handful of carboxylesterase (CES) enzymes in peripheral tissues (Long et al., 2009b). To evaluate whether KML29 also showed improved selectivity against CESs, we performed competitive ABPP experiments in liver, lung, and spleen proteomes. In vitro profiles confirmed the superior selectivity of KML29, which showed much less cross-reactivity with CESs in mouse lung proteomes compared to JZL184 (Figure S2). We also evaluated the peripheral activity and selectivity of JZL184 and KML29 in vivo by analyzing whole-tissue homogenates from inhibitor-treated mice by gel-based ABPP (Figure 3C). Consistent with our previous work, JZL184 inhibited MAGL at low doses (1 mg kg^{-1}) but also displayed significant reactivity with several CESs in the liver, lung, and spleen (Long et al., 2009b). KML29 produced near-complete blockade of MAGL in these peripheral tissues at the lowest dose tested (1 mg kg^{-1}), and, in contrast to JZL184, did not show any detectable CES cross-reactivity until higher doses (20–40 mg/kg), where the blockade of a single ~70 kDa enzyme was detected. This enzyme likely corresponds to carboxylesterase 1 (ES1), which is found abundantly in plasma (Krishnasamy et al., 1998) and exhibits promiscuous reactivity with many carbamates, including JZL184 (Long et al., 2009b; Alexander and Cravatt, 2005; Bachovchin et al., 2010; Chang et al., 2011).

The superior selectivity of KML29 over JZL184 was perhaps most strikingly demonstrated in a chronic dosing study, where the competitive ABPP results were compared for brain and peripheral tissues from mice treated for 6 days with each inhibitor (40 mg kg^{-1}, p.o.). Under this dosing regime, JZL184 not only inhibited MAGL but also FAAH in brain (Figure 4A), as has been reported previously (Schlosburg et al., 2010) as well as several CES enzymes in peripheral tissues (Figures 4B and S3). In contrast, chronic dosing with KML29 selectively inhibited MAGL without any effect on FAAH (Figure 4A) and minimal cross-reactivity with CES enzymes (Figure 4B). The selectivity of KML29 over JZL184 in chronic dosing experiments was further demonstrated by measuring MAGL and FAAH substrate levels in inhibitor-treated mice. KML29 was found to selectively raise 2-AG, but not NAE levels, whereas JZL184 caused increases in both 2-AG and NAEs (Figure 4C). Brain endocannabinoid hydrolytic activities were also measured ex vivo from chronically treated mice revealing that KML29 selectively blocked 2-AG, but not AEA-hydrolysis, whereas JZL184 inhibited both of these activities (Figure 4C).

KML29 Selectively Inhibits Rat and Human Orthologs of MAGL

As has been reported previously (Long et al., 2009b), JZL184 exhibits equivalent potency for mouse and hMAGL, but substantially lower activity against rat MAGL (Figure 5; Table 1). Although the basis for JZL184's reduced potency against rat MAGL remains unknown, we wondered whether KML29 and other HFIP carbamates might show improved activity for this enzyme. Indeed, competitive ABPP analysis of rat brain homogenates revealed that HFIP carbamates retain much of their potency and selectivity for rat MAGL (and rat ABHD6, in the case of JW618) (Figure 5A; Table 1). KML29, for instance, displayed an IC_{50} value of 43 nM for inhibiting rat MAGL (Table 1), which was within approximately 3-fold of its potency for mouse

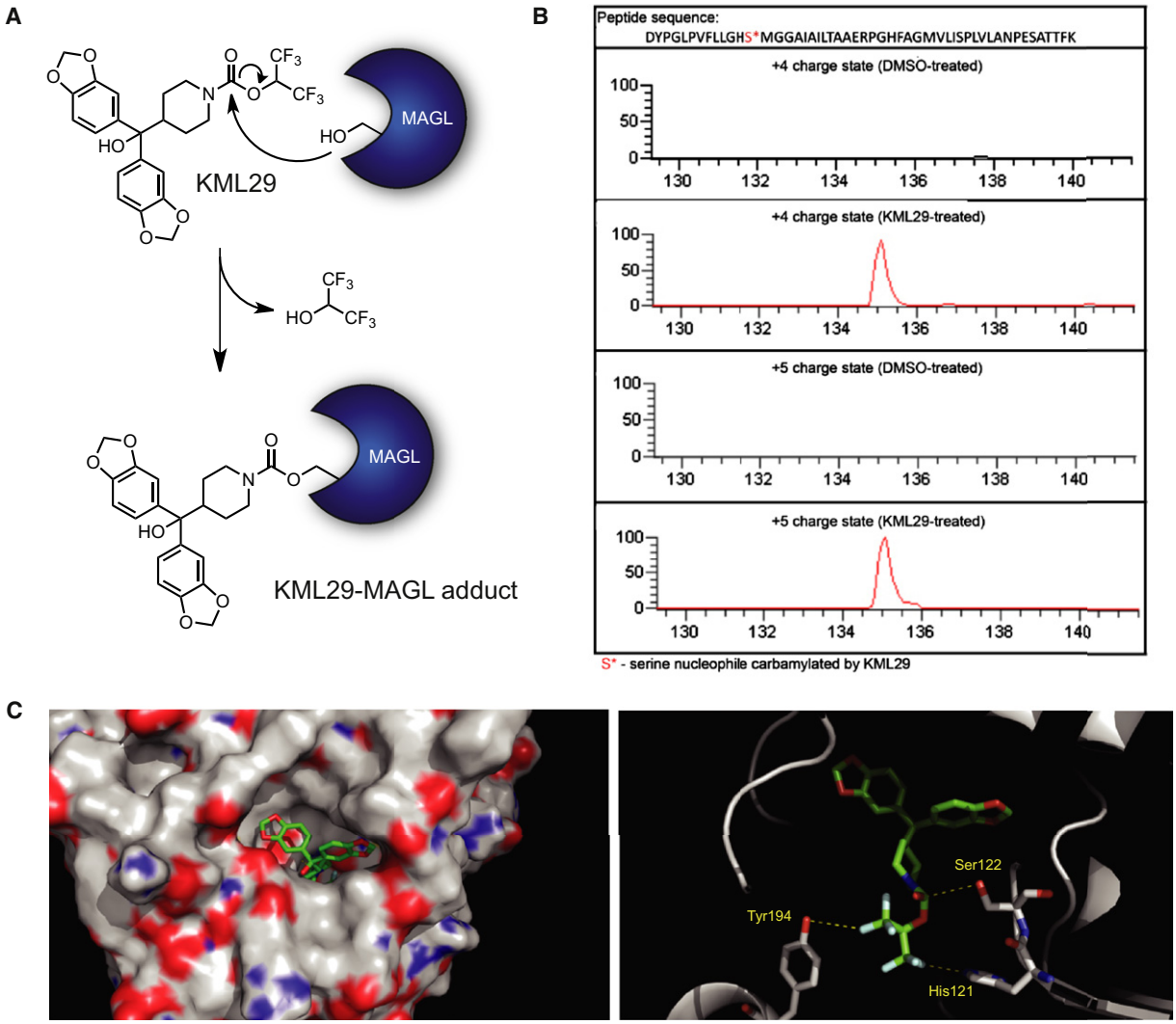

Figure 2. Characterization of KML29-Mediated Inactivation of MAGL

(A) Proposed mechanism of MAGL inactivation by KML29. The catalytic serine (Ser122) of MAGL attacks the activated carbamate of KML29, releasing hexafluoroisopropanol and forming a stable, carbamylated KML29-MAGL covalent adduct.

(B) Extracted ion chromatograms for +4 (m/z = 1408.2310) and +5 (m/z = 1126.7862) charge states corresponding to the KML29-modified adduct of the active site tryptic peptide from DMSO-treated and KML29-treated recombinant, purified hMAGL.

(C) Proposed docking mode of KML29 to MAGL illustrated in views of the whole protein (left image) and the active site (right image). When the catalytic Ser122 is positioned for nucleophilic attack at the carbonyl of KML29, His121 and Tyr194, which are predicted to interact with 2-AG's head group (Bertrand et al., 2010), show potentially favorable interactions with the KML29's HFIP leaving group. RosettaLigand 3.3 (http://www.ncbi.nlm.nih.gov/pubmed/19041878) was used to perform the docking, and the MAGL structure used for docking was 3JWE from the Protein Data Bank (Bertrand et al., 2010).

MAGL (IC_{50} = 15 nM), and maintained good selectivity relative to rat FAAH (no detectable cross-reactivity) and ABHD6 (>20-fold selectivity) (Table 1). We did not detect any additional off target reactivity with other rat brain serine hydrolases for KML29 (Figure 5B) or for JW618 and JW642 (Figure S3).

We next tested whether KML29 could inhibit rat MAGL in vivo. Wistar rats were treated with KML29 (1–40 mg kg^{-1}, i.p.) or vehicle. After 4 hr, each rat was sacrificed, and their tissues were collected for competitive ABPP and lipid analyses. Gel-based ABPP revealed clear dose-dependent inhibition of MAGL in rat brain without any detectable cross-reactivity with FAAH or ABHD6 (Figure 5C). KML29 was slightly less potent in rats than mice, producing >90% inhibition of brain MAGL at 40 mg kg^{-1}. Analysis of peripheral tissues revealed complete MAGL inhibition at 5 mg kg^{-1} in lung and spleen and 20 mg kg^{-1} in liver (Figure S3). As was observed in mice, only one off target was detected for KML29 in peripheral tissues of rat by competitive ABPP, a 70 kDa serine hydrolase that is likely the rat ortholog of ES1.

Analysis of brain lipids corroborated our competitive ABPP results, revealing approximately 10-fold elevations in 2-AG without alteration of AEA, PEA, or OEA (Figure 5D). We also measured brain 2-AG hydrolytic activity, which was diminished by 50% at 20 mg kg^{-1} and 80% at 40 mg kg^{-1} doses of

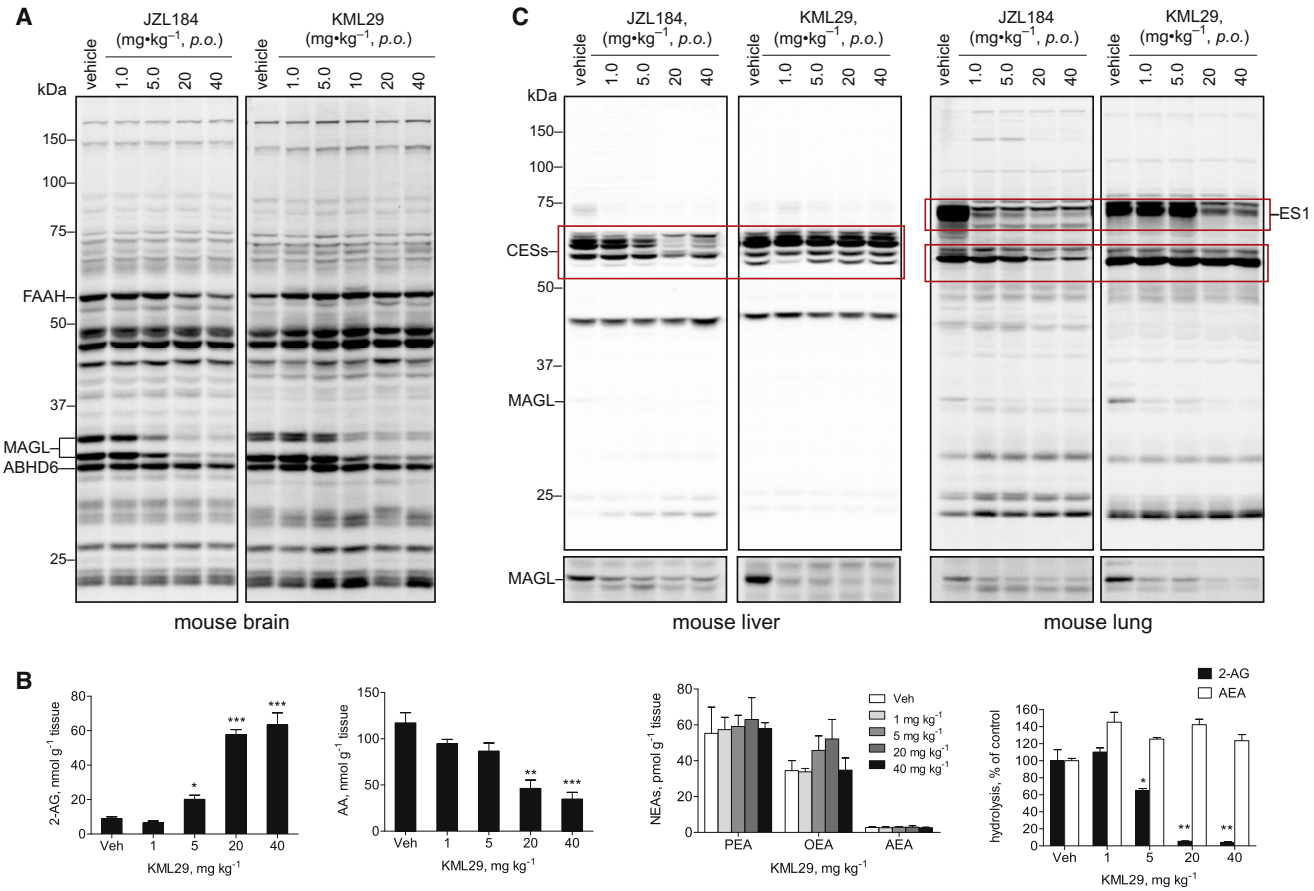

Figure 3. In Vivo Characterization of KML29 Activity in Mice

(A) Competitive ABPP gel of FP-Rh labeling of brain serine hydrolase activities from mice treated with JZL184 or KML29 at the indicated dose (1–40 mg kg^{-1}, p.o.) for 4 hr.

(B) Brain lipid profile for 2-AG, AA, AEA, PEA, OEA across the indicated dose range of KML29 (p.o.). 2-AG and AEA hydrolytic activity of brain tissue isolated from KML29 treated mice (far right graph).

(C) Competitive ABPP gels of serine hydrolase activities in liver and lung tissues from mice treated with either JZL184 or KML29 (1–40 mg kg^{-1}, p.o.) for 4 hr. Boxes mark various CES enzymes that show differential sensitivity to JZL184 versus KML29. Also see Figure S2 for in vitro inhibition of CESs by JZL184 and KML29 in lung proteomes and ABPP gels from spleen proteomes isolated from mice treated with JZL184 and KML29.

Data are presented as mean ± SEM (n = 3 mice per group). *p < 0.05; **p < 0.01; ***p < 0.001 for vehicle-treated versus inhibitor-treated mice.

See also Figure S2.

KML29 (Figure 5E). Because ABHD6 and ABHD12 can also hydrolyze 2-AG (Blankman et al., 2007), it is plausible that the remaining 20% 2-AG hydrolytic activity in rat brain is due to these enzymes, which were not inhibited by KML29 in vivo. Brain AEA hydrolytic activity, on the other hand, was not affected at any dose of KML29 (Figure 5E). Finally, brain AA levels were found to decrease proportionally with the elevations in 2-AG caused by KML29 treatment (Figure 5D). Together, these data indicate that KML29 offers a selective, in vivo-active probe for investigating MAGL function in rats, an objective that has not been straightforward to achieve with past inhibitors.

Endocannabinoid hydrolase inhibitors have therapeutic potential for treating a range of human disorders. Rodent studies have revealed, however, that dual inhibitors of FAAH and MAGL produce psychotropic effects that resemble the activity of direct cannabinoid agonists (Long et al., 2009c). It is therefore important that inhibitors maintain excellent selectivity for hMAGL compared to human FAAH (hFAAH). By performing competitive ABPP assays with cell lysates from HEK293T cells transiently transfected with hMAGL or hFAAH cDNAs, we found that KML29 inhibited hMAGL with an IC_{50} value of 5.9 nM, while showing no detectable cross-reactivity with hFAAH (Figure 5F). Other HFIP carbamates also showed excellent potency for hMAGL and maintained high selectivity over hFAAH (Figure 5F). We should further note that JZL184 itself displayed striking selectivity for hMAGL, exhibiting no detectable cross-reactivity with FAAH up to 50 μM (Figure 5F). Finally, we also measured the inhibition of hMAGL and hFAAH by KML29 using substrate hydrolysis assays, which revealed subnanomolar inhibition of 2-AG hydrolysis (IC_{50} = 0.14 nM) and undiminished AEA hydrolysis up to 50 μM (Figure 5F). The lower IC_{50} value calculated by substrate compared to competitive ABPP assays may reflect titration of MAGL protein in the latter format, which used higher concentrations of protein

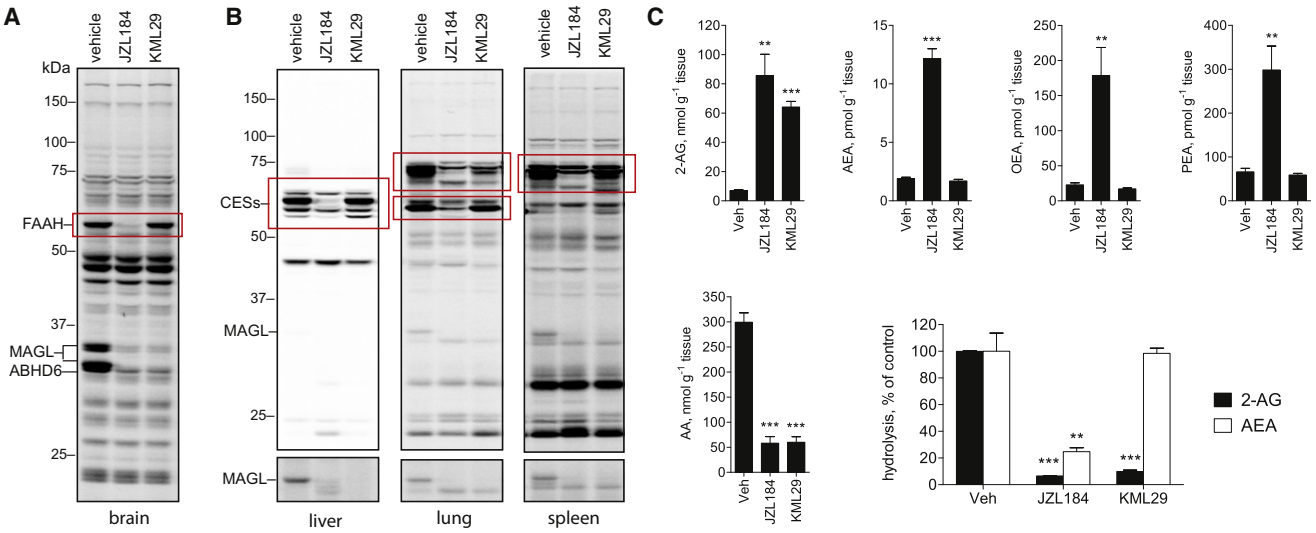

Figure 4. Characterization of Serine Hydrolase Activities and Endocannabinoid Metabolism in Mice Treated Chronically with KML29 and JZL184

(A) Competitive ABPP gels of serine hydrolase activities in brain from mice chronically treated with vehicle, JZL184, or KML29 (40 mg kg^{-1} day^{-1}, p.o., 6 days).

(B) Competitive ABPP gels of serine hydrolase activities in liver, lung, and spleen from mice chronically treated with vehicle, JZL184, or KML29. Boxes mark various off targets that show differential sensitivity to JZL184 versus KML29.

(C) Brain lipid profiles and endocannabinoid hydrolytic activities measured from mice chronically treated with vehicle, JZL184, or KML29.

Data are presented as means ± SEM (n = 3 mice per group). *p < 0.05; **p < 0.01; ***p < 0.001 for vehicle-treated versus inhibitor-treated mice.

for analysis (0.01 versus 0.1 mg MAGL-transfected cell proteome/ml, respectively).

DISCUSSION

The development of selective, in vivo-active chemical probes is often the catalyst for groundbreaking discoveries in mammalian biology (Moellering and Cravatt, 2012; Edwards et al., 2011). An historical look at endocannabinoid research bears this out when considering the mechanistic insights that have been gained following the development of selective receptor agonists and antagonists, as well as inhibitors of endocannabinoid hydrolases (Ligresti et al., 2009; Graham et al., 2009; Di Marzo, 2008, 2009; De Petrocellis and Di Marzo, 2009; Fowler, 2008; Ahn et al., 2008; Guindon et al., 2011). Selective FAAH inhibitors have existed for at least a decade (Boger et al., 2000; Kathuria et al., 2003), whereas selective MAGL inhibitors, such as JZL184 (Long et al., 2009a, 2010), have emerged only in the last few years. Even within this short time period, MAGL inhibitors have already played a key part in the discovery of MAGL's role in processes such as pain (Long et al., 2009a; Kinsey et al., 2009), neuropsychiatric disorders (Sciolino et al., 2011; Busquets-Garcia et al., 2011), cancer (Nomura et al., 2010, 2011a), and neuroinflammation (Nomura et al., 2011b). Notwithstanding the impact that JZL184 has had on our understanding of MAGL function in mammalian biology, some limitations have constrained the utility of this agent and have encouraged us to develop inhibitors with improved specificity. Of primary concern was the low-level cross-reactivity that JZL184 displays for FAAH, which becomes problematic in studies that require high doses or chronic administration of the inhibitor (Long et al., 2009a, 2009b; Schlosburg et al., 2010). Because simultaneous inhibition of MAGL and FAAH elicits a unique subset of behaviors distinct from those caused by inhibition of either FAAH or MAGL alone (Long et al., 2009a), it is imperative that FAAH cross-reactivity is avoided to allow for accurate assignment of MAGL-mediated biological effects. JZL184 also inactivates a handful of CES enzymes (Long et al., 2009b), which complicates the use of this inhibitor to investigate peripheral functions of MAGL. With these considerations in mind, we report herein a class of MAGL inhibitors, the HFIP carbamates, which exhibit vastly improved selectivity for MAGL in both the brain and peripheral tissues.

We selected HFIP carbamates because they possess a leaving group with a pKa value that is comparable to that of *p*-nitrophenol, the leaving group of JZL184. We also envisioned that the HFIP group would serve as an activated isostere of the 2-AG head group and, because of its increased size, might impart additional selectivity for FAAH, which is particularly sensitive to head group sterics (Lang et al., 1999). These hypotheses were confirmed through the generation of KML29, an HFIP analog of JZL184 that maintained the original inhibitor's potency for MAGL while showing greatly improved selectivity over FAAH and CES enzymes. Even incorporation of the HFIP group into a potent FAAH inhibitor like JZL195 converted this agent into an MAGL/ABHD6 selective inhibitor JW642 that showed no observable FAAH reactivity up to 10 μM. It should be emphasized that, in general, the MAGL/ABHD6 selectivity ratios were not altered by incorporation of the HFIP group, suggesting that ABHD6 selectivity is driven primarily by the amine portion of the tested carbamates. Our competitive ABPP assays also did not uncover any additional off targets for HFIP carbamates across the serine hydrolase class (other than ES1), although deeper profiling by mass spectrometry methods (Jessani et al., 2005) will be required to more fully explore the proteome-wide

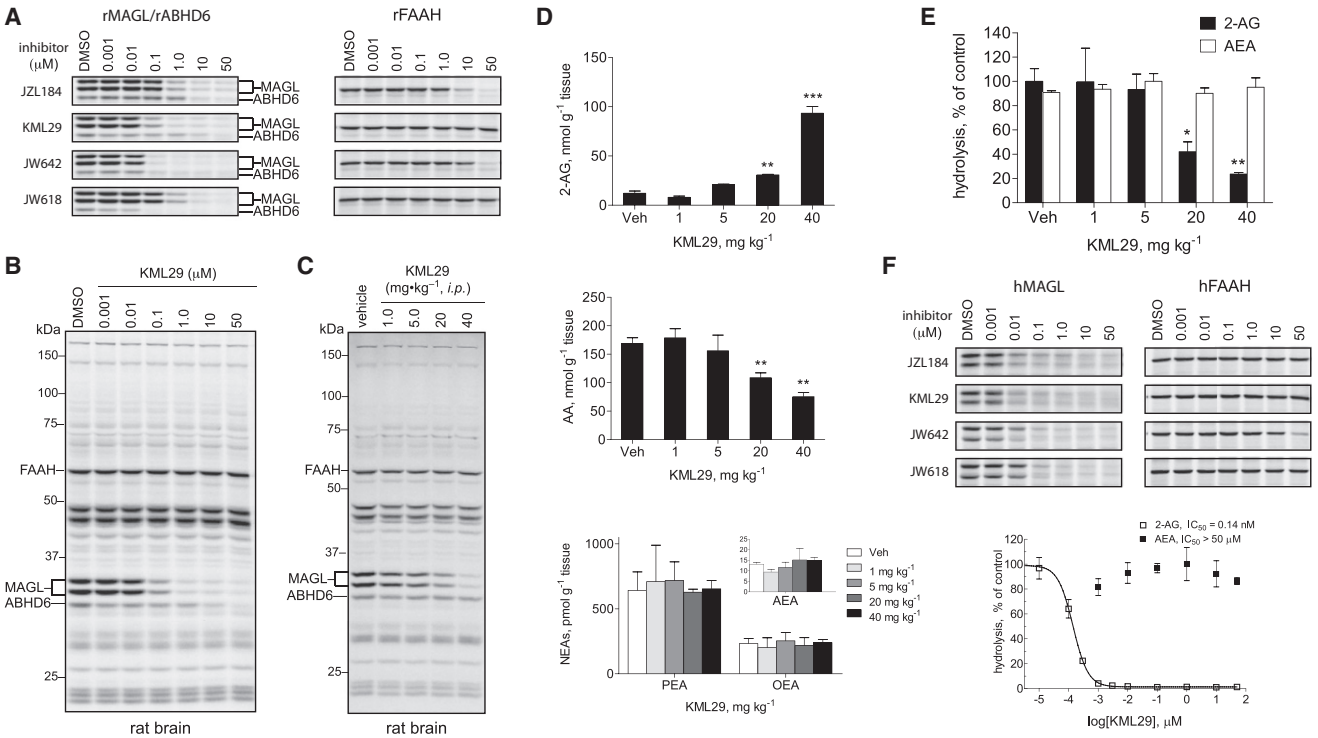

Figure 5. Inhibition of Rat and Human MAGL Enzymes by KML29

(A) Competitive ABPP gels comparing the potency and selectivity of JZL184, KML29, JW642, and JW618 against MAGL, ABHD6, and FAAH in rat brain proteomes. See Figure S3 for full gel profiles of each inhibitor. See also Table 1 for IC_{50} values calculated from gel-based ABPP experiments.

(B) Full competitive ABPP gel showing KML29 activity against rat brain serine hydrolase activities, which revealed selective inhibition of MAGL at inhibitor concentrations of 1 μM or less and inhibition of ABHD6 at concentrations >1 μM. No inhibition of FAAH was detected at any tested concentration of KML29.

(C) Competitive ABPP gel of brain serine hydrolase activities from rats treated with KML29 (1–40 mg kg^{-1}, i.p.) for 4 hr. Also see Figure S3 for gel profiles of liver, lung, and spleen from rats treated with KML29.

(D) Brain lipid profile of 2-AG, AA, AEA, PEA, OEA from rats treated with KML29 (1–40 mg kg^{-1}, i.p.).

(E) Brain MAGL and FAAH activity from rats treated with KML29 (1–40 mg kg^{-1}, i.p.) as measured by 2-AG and AEA hydrolysis, respectively.

(F) Activity of JZL184, KML29, JW642, and JW618 against recombinant hMAGL and hFAAH by gel-based competitive ABPP (upper gel panels) and substrate hydrolysis assay for KML29 (lower graph). See also Table 1 for IC_{50} values calculated from gel-based ABPP experiments.

Data are presented as mean ± SEM (n = 3 rats per group). *p < 0.05; **p < 0.01; ***p < 0.001 for vehicle-treated versus inhibitor-treated rats.

See also Figure S3.

selectivity of these agents. These results, taken together, designate HFIP carbamates as a useful scaffold for inhibiting the 2-AG hydrolases MAGL and ABHD6.

We found that KML29 selectively inactivated MAGL in vivo without any detectable FAAH inhibition across the entire tested dose range. This selectivity was reflected not only in measurements of enzyme activity but also in brain lipid profiles, where KML29 produced ~10-fold elevations in 2-AG (and reductions in AA) without alteration in FAAH substrates, AEA, OEA, or PEA. KML29 proved active in both mouse and rat, thus offering a more versatile chemical probe than JZL184 for exploring a range of rodent behavioral models. The superior selectivity of KML29 relative to JZL184 was also confirmed in vivo using both acute and chronic dosing regimes (Figures 3 and 4). Finally, we found that HFIP carbamates also display excellent potency and specificity for hMAGL, suggesting that they could offer a useful starting point for the development of therapeutic agents. On this note, we were gratified to identify doses where KML29 produced partial inhibition of brain MAGL (as reflected in both enzyme activity and brain lipid measurements; see Figures 3 and 5) because complete blockade of this enzyme is known to produce tolerance and desensitization of CB1 receptors in mice (Schlosburg et al., 2010).

SIGNIFICANCE

Monoacylglycerol lipase (MAGL), through catalyzing the hydrolysis of 2-arachidonoyl glycerol to arachidonic acid, serves as a key metabolic hub connecting the endocannabinoid and eicosanoid signaling networks. Small-molecule inhibitors that selectively target MAGL are critical tools for unraveling the functions and crosstalk between these two lipid transmitters systems, and hold potential for treating a wide spectrum of disorders, including anxiety, pain, inflammation, and cancer. We report herein a class of MAGL inhibitors, *O*-hexafluoroisopropyl (HFIP) carbamates, that displays excellent potency and in vivo activity and, in comparison to previously described *O*-aryl carbamates, greatly enhanced selectivity over fatty acid amide hydrolase and other serine hydrolases. That HFIP carbamates appear

to achieve their potency and selectivity for MAGL (and ABHD6) at least in part due to the bioisosteric nature of their leaving group leads us to speculate that this type of substrate-mimetic strategy for covalent inhibitor design could be generalized to develop useful probes for many additional serine hydrolases.

EXPERIMENTAL PROCEDURES

Materials

All commercially available chemicals were obtained from Sigma-Aldrich, Acros, Fisher, Fluka, or Maybridge and were used without further purification, except where noted. FP-rhodamine (Patricelli et al., 2001) and JZL184 (Long et al., 2009a) were prepared according the previously reported methods. Detailed synthetic procedures and experimental data for KML29, JW642, and JW618 are provided in the Supplemental Information. LC/MS lipid standards were purchased from Cayman Chemical.

In Vitro Competitive Activity-Based Protein Profiling

Proteomes (brain membrane fraction or cell lysates) (50 μl, 1.0 mg/ml total protein concentration) were preincubated with varying concentrations of inhibitors at 37°C. After 30 min, FP-Rh (1.0 μl, 50 μM in DMSO) was added, and the mixture was incubated for another 30 min at room temperature. Reactions were quenched with 4× SDS loading buffer (17 μl) and run on SDS-PAGE. Following gel imaging, serine hydrolase activity was determined by measuring fluorescent intensity of gel bands corresponding to MAGL, ABHD6, and FAAH using ImageJ 1.43u software.

In Vivo Administration of KML29

For intraperitoneal injections, KML29 was prepared as an emulsion in saline:emulphor:ethanol by first adding a 1:1 mixture of ethanol:emulphor and sonicating for 1 h with gentle heating (~50°C) and subsequently diluting this cloudy mixture with saline to a final saline:emulphor:ethanol ratio of 18:1:1. For oral administration, KML29 was dissolved in PEG300 (Fluka) by sonicating for 1 h with gentle heating. KML29 was administered to either C57Bl/6J mice or Wistar rats in a vehicle of either saline:emulphor:ethanol (18:1:1) for intraperitoneal injections or PEG300 for administration by oral gavage. After the indicated dosing regimens, the animals were anesthetized using isoflurane or CO_2 and sacrificed by decapitation and tissues were immediately frozen in liquid N_2. Each organ was washed with cold phosphate-buffered saline at 0°C (3 × 2 ml) to remove excess blood and immediately dounce homogenized in PBS (1 ml). Dounced tissue was sonicated and centrifuged (3000 rpm, 3 min, 4°C) to remove cellular debris. Brain homogenates were further centrifuged at high speed (100,000*g*, 45 min, 4°C) to separate membrane and soluble cell components. The supernatant was removed and the remaining pellet was gently washed with cold PBS (2 × 500 μl) and sonicated in PBS (500 μl) to resuspend. Total protein concentrations of tissue proteomes were determined using the Bio-Rad DC Protein Assay kit. Proteomic mixtures were either diluted to 1.0 mg/ml total protein concentration with PBS for immediate use or aliquoted and stored at −80°C. The studies were performed with the approval of the Institutional Animal Care and Use Committee at The Scripps Research Institute in accordance with the Guide for the Care and Use of Laboratory Animals.

Recombinant Expression of Human MAGL in HEK293T Cells

hMAGL and hFAAH were expressed in HEK293T cells according to previously reported methods (Blankman et al., 2007). Cell lysates were diluted with mock proteomes for use in competitive ABPP experiments.

Measurement of Brain Lipids

Brain lipid levels were determined according to previously reported methods (Long et al., 2009c).

Enzyme Activity Assays

MAGL and FAAH substrate hydrolysis measurements were determined according to the previously reported LC-MS-based assay (Long et al., 2009a, 2009c).

Expression and Purification of Recombinant Human MAGL

hMAGL was expressed in BL21(DE3) cells (Invitrogen) and purified according to previously reported methods (Long et al., 2009b).

Detection of KML29-MAGL Adduct from KML29-Treated Preparations of hMAGL

Tryptic digests of KML29 or DMSO-treated recombinant hMAGL were analyzed using an LTQ-Orbitrap mass spectrometer (ThermoFisher) coupled to an Agilent 1100 series HPLC. Labeling, sample preparation, and LC-MS/MS analysis were performed in accordance with previously reported methods (Long et al., 2009b).

Docking Method

The ligand structure of KML29 was generated using Chem3D (http://www.cambridgesoft.com), and the protein structure was taken from the crystal structure of MAGL with covalent inhibitor SAR629 (PDB code: 3JWE). RosettaLigand 3.3 (Davis and Baker, 2009) was used to perform the docking study. The starting docking pose was created by aligning KML29 to the position of SAR629 in the 3JWE structure and local docking perturbation with translation and rotation magnitude of 3.0 Å and 30° was performed in all-atom mode to generate ~11,500 models. A distance constraint (<3.5 Å) between the hydroxyl oxygen of Ser132 and the carbonyl carbon of KML29 was implemented to filter out any unsatisfying models that do not sterically support the nucleophilic attack to the catalytic serine to the substrate ester. Final models were visually inspected and analyzed. Figures were illustrated using PyMOL (http://www.pymol.org).

SUPPLEMENTAL INFORMATION

Supplemental Information includes three figures, Supplemental Experimental Procedures, and synthetic procedures and full characterization for compounds KML29, JW642, and JW618 and can be found with this article online at doi:10.1016/j.chembiol.2012.03.009.

ACKNOWLEDGMENTS

This work was supported by the National Institutes of Health Grants DA017259 (to B.F.C.), DA009789 (to B.F.C.), and DA032541 (to M.J.N.) and the Skaggs Institute for Chemical Biology. B.F.C. is a founder of Abide Therapeutics and a member of its scientific advisory board. This work was supported in part by a grant from Abide Therapeutics.

Received: February 8, 2012
Revised: March 20, 2012
Accepted: March 26, 2012
Published online: April 26, 2012

REFERENCES

Ahn, K., McKinney, M.K., and Cravatt, B.F. (2008). Enzymatic pathways that regulate endocannabinoid signaling in the nervous system. Chem. Rev. *108*, 1687–1707.

Ahn, K., Johnson, D.S., Mileni, M., Beidler, D., Long, J.Z., McKinney, M.K., Weerapana, E., Sadagopan, N., Liimatta, M., Smith, S.E., et al. (2009). Discovery and characterization of a highly selective FAAH inhibitor that reduces inflammatory pain. Chem. Biol. *16*, 411–420.

Alexander, J.P., and Cravatt, B.F. (2005). Mechanism of carbamate inactivation of FAAH: implications for the design of covalent inhibitors and *in vivo* functional probes for enzymes. Chem. Biol. *12*, 1179–1187.

Bachovchin, D.A., Ji, T., Li, W., Simon, G.M., Blankman, J.L., Adibekian, A., Hoover, H., Niessen, S., and Cravatt, B.F. (2010). Superfamily-wide portrait of serine hydrolase inhibition achieved by library-versus-library screening. Proc. Natl. Acad. Sci. USA *107*, 20941–20946.

Bertrand, T., Augé, F., Houtmann, J., Rak, A., Vallée, F., Mikol, V., Berne, P.F., Michot, N., Cheuret, D., Hoornaert, C., and Mathieu, M. (2010). Structural basis for human monoglyceride lipase inhibition. J. Mol. Biol. *396*, 663–673.

Blankman, J.L., Simon, G.M., and Cravatt, B.F. (2007). A comprehensive profile of brain enzymes that hydrolyze the endocannabinoid 2-arachidonoylglycerol. Chem. Biol. *14*, 1347–1356.

Boger, D.L., Sato, H., Lerner, A.E., Hedrick, M.P., Fecik, R.A., Miyauchi, H., Wilkie, G.D., Austin, B.J., Patricelli, M.P., and Cravatt, B.F. (2000). Exceptionally potent inhibitors of fatty acid amide hydrolase: the enzyme responsible for degradation of endogenous oleamide and anandamide. Proc. Natl. Acad. Sci. USA *97*, 5044–5049.

Busquets-Garcia, A., Puighermanal, E., Pastor, A., de la Torre, R., Maldonado, R., and Ozaita, A. (2011). Differential role of anandamide and 2-arachidonoylglycerol in memory and anxiety-like responses. Biol. Psychiatry *70*, 479–486.

Chang, J.W., Nomura, D.K., and Cravatt, B.F. (2011). A potent and selective inhibitor of KIAA1363/AADACL1 that impairs prostate cancer pathogenesis. Chem. Biol. *18*, 476–484.

Cravatt, B.F., Demarest, K., Patricelli, M.P., Bracey, M.H., Giang, D.K., Martin, B.R., and Lichtman, A.H. (2001). Supersensitivity to anandamide and enhanced endogenous cannabinoid signaling in mice lacking fatty acid amide hydrolase. Proc. Natl. Acad. Sci. USA *98*, 9371–9376.

Davis, I.W., and Baker, D. (2009). RosettaLigand docking with full ligand and receptor flexibility. J. Mol. Biol. *385*, 381–392.

De Petrocellis, L., and Di Marzo, V. (2009). An introduction to the endocannabinoid system: from the early to the latest concepts. Best Pract. Res. Clin. Endocrinol. Metab. *23*, 1–15.

Di Marzo, V. (2008). Targeting the endocannabinoid system: to enhance or reduce? Nat. Rev. Drug Discov. *7*, 438–455.

Di Marzo, V. (2009). The endocannabinoid system: its general strategy of action, tools for its pharmacological manipulation and potential therapeutic exploitation. Pharmacol. Res. *60*, 77–84.

Edwards, A.M., Isserlin, R., Bader, G.D., Frye, S.V., Willson, T.M., and Yu, F.H. (2011). Too many roads not taken. Nature *470*, 163–165.

Fowler, C.J. (2008). "The tools of the trade"—an overview of the pharmacology of the endocannabinoid system. Curr. Pharm. Des. *14*, 2254–2265.

Graham, E.S., Ashton, J.C., and Glass, M. (2009). Cannabinoid receptors: a brief history and "what's hot". Front. Biosci. *14*, 944–957.

Guindon, J., Guijarro, A., Piomelli, D., and Hohmann, A.G. (2011). Peripheral antinociceptive effects of inhibitors of monoacylglycerol lipase in a rat model of inflammatory pain. Br. J. Pharmacol. *163*, 1464–1478.

Jessani, N., Niessen, S., Wei, B.Q., Nicolau, M., Humphrey, M., Ji, Y., Han, W., Noh, D.Y., Yates, J.R., 3rd, Jeffrey, S.S., and Cravatt, B.F. (2005). A streamlined platform for high-content functional proteomics of primary human specimens. Nat. Methods *2*, 691–697.

Karlsson, M., Reue, K., Xia, Y.-R., Lusis, A.J., Langin, D., Tornqvist, H., and Holm, C. (2001). Exon-intron organization and chromosomal localization of the mouse monoglyceride lipase gene. Gene *272*, 11–18.

Kathuria, S., Gaetani, S., Fegley, D., Valiño, F., Duranti, A., Tontini, A., Mor, M., Tarzia, G., La Rana, G., Calignano, A., et al. (2003). Modulation of anxiety through blockade of anandamide hydrolysis. Nat. Med. *9*, 76–81.

Kinsey, S.G., Long, J.Z., O'Neal, S.T., Abdullah, R.A., Poklis, J.L., Boger, D.L., Cravatt, B.F., and Lichtman, A.H. (2009). Blockade of endocannabinoid-degrading enzymes attenuates neuropathic pain. J. Pharmacol. Exp. Ther. *330*, 902–910.

Krishnasamy, S., Teng, A.L., Dhand, R., Schultz, R.M., and Gross, N.J. (1998). Molecular cloning, characterization, and differential expression pattern of mouse lung surfactant convertase. Am. J. Physiol. *275*, L969–L975.

Lang, W., Qin, C., Lin, S., Khanolkar, A.D., Goutopoulos, A., Fan, P., Abouzid, K., Meng, Z., Biegel, D., and Makriyannis, A. (1999). Substrate specificity and stereoselectivity of rat brain microsomal anandamide amidohydrolase. J. Med. Chem. *42*, 896–902.

Leung, D., Hardouin, C., Boger, D.L., and Cravatt, B.F. (2003). Discovering potent and selective reversible inhibitors of enzymes in complex proteomes. Nat. Biotechnol. *21*, 687–691.

Li, W., Blankman, J.L., and Cravatt, B.F. (2007). A functional proteomic strategy to discover inhibitors for uncharacterized hydrolases. J. Am. Chem. Soc. *129*, 9594–9595.

Lichtman, A.H., Shelton, C.C., Advani, T., and Cravatt, B.F. (2004). Mice lacking fatty acid amide hydrolase exhibit a cannabinoid receptor-mediated phenotypic hypoalgesia. Pain *109*, 319–327.

Ligresti, A., Petrosino, S., and Di Marzo, V. (2009). From endocannabinoid profiling to 'endocannabinoid therapeutics'. Curr. Opin. Chem. Biol. *13*, 321–331.

Long, J.Z., Li, W., Booker, L., Burston, J.J., Kinsey, S.G., Schlosburg, J.E., Pavón, F.J., Serrano, A.M., Selley, D.E., Parsons, L.H., et al. (2009a). Selective blockade of 2-arachidonoylglycerol hydrolysis produces cannabinoid behavioral effects. Nat. Chem. Biol. *5*, 37–44.

Long, J.Z., Nomura, D.K., and Cravatt, B.F. (2009b). Characterization of monoacylglycerol lipase inhibition reveals differences in central and peripheral endocannabinoid metabolism. Chem. Biol. *16*, 744–753.

Long, J.Z., Nomura, D.K., Vann, R.E., Walentiny, D.M., Booker, L., Jin, X., Burston, J.J., Sim-Selley, L.J., Lichtman, A.H., Wiley, J.L., and Cravatt, B.F. (2009c). Dual blockade of FAAH and MAGL identifies behavioral processes regulated by endocannabinoid crosstalk *in vivo*. Proc. Natl. Acad. Sci. USA *106*, 20270–20275.

Long, J.Z., Jin, X., Adibekian, A., Li, W., and Cravatt, B.F. (2010). Characterization of tunable piperidine and piperazine carbamates as inhibitors of endocannabinoid hydrolases. J. Med. Chem. *53*, 1830–1842.

Marrs, W.R., Blankman, J.L., Horne, E.A., Thomazeau, A., Lin, Y.H., Coy, J., Bodor, A.L., Muccioli, G.G., Hu, S.S., Woodruff, G., et al. (2010). The serine hydrolase ABHD6 controls the accumulation and efficacy of 2-AG at cannabinoid receptors. Nat. Neurosci. *13*, 951–957.

Moellering, R.E., and Cravatt, B.F. (2012). How chemoproteomics can enable drug discovery and development. Chem. Biol. *19*, 11–22.

Nomura, D.K., Long, J.Z., Niessen, S., Hoover, H.S., Ng, S.W., and Cravatt, B.F. (2010). Monoacylglycerol lipase regulates a fatty acid network that promotes cancer pathogenesis. Cell *140*, 49–61.

Nomura, D.K., Lombardi, D.P., Chang, J.W., Niessen, S., Ward, A.M., Long, J.Z., Hoover, H.H., and Cravatt, B.F. (2011a). Monoacylglycerol lipase exerts dual control over endocannabinoid and fatty acid pathways to support prostate cancer. Chem. Biol. *18*, 846–856.

Nomura, D.K., Morrison, B.E., Blankman, J.L., Long, J.Z., Kinsey, S.G., Marcondes, M.C.G., Ward, A.M., Hahn, Y.K., Lichtman, A.H., Conti, B., and Cravatt, B.F. (2011b). Endocannabinoid hydrolysis generates brain prostaglandins that promote neuroinflammation. Science *334*, 809–813.

Patricelli, M.P., Giang, D.K., Stamp, L.M., and Burbaum, J.J. (2001). Direct visualization of serine hydrolase activities in complex proteomes using fluorescent active site-directed probes. Proteomics *1*, 1067–1071.

Schlosburg, J.E., Blankman, J.L., Long, J.Z., Nomura, D.K., Pan, B., Kinsey, S.G., Nguyen, P.T., Ramesh, D., Booker, L., Burston, J.J., et al. (2010). Chronic monoacylglycerol lipase blockade causes functional antagonism of the endocannabinoid system. Nat. Neurosci. *13*, 1113–1119.

Sciolino, N.R., Zhou, W., and Hohmann, A.G. (2011). Enhancement of endocannabinoid signaling with JZL184, an inhibitor of the 2-arachidonoylglycerol hydrolyzing enzyme monoacylglycerol lipase, produces anxiolytic effects under conditions of high environmental aversiveness in rats. Pharmacol. Res. *64*, 226–234.

